# Analytical Methods

Accepted Manuscript


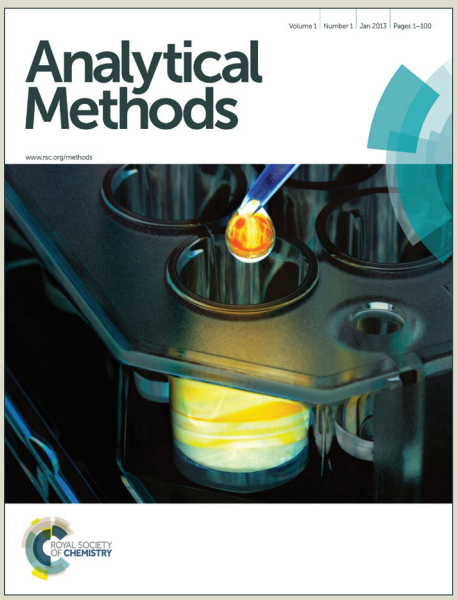





ROYAL SOCIETY OF CHEMISTRY

www.rsc.org/methods

# Development and validation of dot-ELISA on modified cellulose filter paper: A simplified novel approach

Charu Tyagi [1,2,3,*], Lomas K. Tomar [1], Pradeep Kumar[1], Viness Pillay[1] and Harpal Singh[3,*]

[1]Department of Pharmacy and Pharmacology, Faculty of Health Sciences, University of the Witwatersrand, 7 York Road, Parktown 2193, Johannesburg, South Africa

[2]V.S.P.G.(P.G) College, C.C.S University, Meerut 250004, U.P., India

[3]Centre for Biomedical Engineering, Indian Institute of Technology, Delhi 110016, India

*Corresponding Authors:

Charu Tyagi
Faculty of Health Sciences
University of the Witwatersrand, Johannesburg, South Africa
Email: tyagi.charu@gmail.com
Tel: +27-11-717-2541, +27-767978187

Harpal Singh
Centre for Biomedical Engineering,
Indian Institute of Technology Delhi, New Delhi, India
Email: harpal2000@yahoo.com

## Abstract

Graft polymerization of glycidyl methacrylate (GMA) onto cellulose filter paper (CFP) was carried out by free-radical polymerization process and grafted surfaces were characterized by standard polymer characterization techniques. Reactional profiles of GMA and cellulose were elucidated using molecular mechanics energy relationships by exploring the spatial disposition of molecular entities. CFP-g-GMA surfaces with different graft levels of GMA were evaluated and standardized for their application in dot-ELISA in two steps. In the first step, sensitivity, specificity and reproducibility of the assay on GMA grafted cellulose surface was evaluated through a model system using rabbit anti-goat IgG, goat anti-rabbit IgG and goat anti-rabbit IgG HRP-conjugate. Variety of blocking agents and different levels of conjugate dilutions were screened to standardize the assay. Rabbit-anti-goat IgG antibody at a concentration as low as 6ngmL$^{-1}$ was efficiently detected on CFP with 70% GMA graft level using 5% skimmed milk as blocking agent and antispecies-IgG-peroxidase conjugate diluted 2000 times. In the second step, sensitivity and specificity of the developed system was established with human blood and finally used to identify the source of mosquito blood meal, an important parameter in epidemiological studies, particularly in determining the role of mosquito in malaria transmission. Time duration of standardized assay reduced to 90 min compared to 3-4 h of usual dot-ELISA. For mass screening, as for epidemiological studies in field conditions, sheet of higher dimensions – instead of small strips as utilized by the researchers for laboratory studies – can be used for multiple spotting.


**Keywords:** *Dot-enzyme linked immunosorbent assay; Glycidyl methacrylate; Cellulose filter paper; Blocking agents; Mosquito blood meal; Molecular mechanics energy relationships.*

## 1. Introduction

Immunodiagnostic methods have long been used in the diagnosis of various diseases. Among these, the solid phase – heterogeneous – immunoenzymatic (IE) assays have become one of the most powerful tools for the laboratory diagnosis of infectious diseases, autoimmune disorders, immune allergies and neoplastic diseases. Such immunoassays require a solid phase, to which are adsorbed the antigen/antibody that recognizes and binds to its complementary antibody/antigen in the sample. The result of binding reaction between the antibody and analyte (antigen) is made visible by means of enzymatic markers.[1] These solid phase IE assays include conventional ELISA (enzyme linked immunosorbent assay) and dot-ELISA which generally utilizes polystyrene (PS) plates and nitrocellulose (NC) membrane, respectively, as the solid phase, to which the adsorption of biomolecules is due to intermolecular attraction forces.[2-4] But these adsorption based procedures suffer from non-specific binding and desorption of biomolecules during incubation and washing steps.[5] It has also been observed that short peptides often do not bind well to the surface of PS-based microtiter plates in solid phase immunoassay.[6,7] In addition, PS plates pose an environmental hazard as, although being disposable, they produce huge amount of carbon monoxide and other toxic gases during incineration due to thermal degradation of PS.[8,9] Modified PS plates, developed and reported by a number of research groups to overcome some of the problems, still have certain drawbacks.[7,10,11] NC membrane on the other hand is costly and requires surface treatment for better attachment of immunoreactants.[12]

A range of synthetic (polypropylene, PS, nylon) and natural polymers (chitosan and cotton) have long been investigated for their use as matrix and support material for enzyme immobilization and in immunoassays.[2,5,13-16] However, in recent years there has been considerable interest and stress on the use of biodegradable polymers. Different polymers, apart from chitosan and cotton, are therefore being explored and applied after suitable modification to have potential end use in these areas. A highly selective glucose biosensor has been prepared by immobilization of glucose oxidase on biodegradable γ–polyglutamic acid film.[17] Microtiter plates based on renewable resource, polylactic acid (PLA) have been patented and launched recently. These are reported to be fully biodegradable and possess an antigen binding efficiency equally well or better than conventionally used polystyrene.[8] An innovative immunostick-cuvette-system has also been reported, in which the stick is made of

the renewable poly(hydroxybutyrate).[8] Cellulose derivatives with different surface properties that has been used as matrix support include cellulose acetate, amino cellulose acetate, cellulose nitrate, etc.[18-20]

Filter paper, a form of cellulose - a natural carbohydrate polymer - is an inexpensive, easily available, degradable and renewable biopolymer with very good mechanical properties. However, its application in several technologically important fields is limited due to the lack of reactive functional sites and thus the desirable surface properties. The use of cellulose-based materials could thus be extended to new areas by altering and tailoring its chemical and physical properties through the incorporation of functional moieties onto its surface. Grafting is one of the promising and attractive methods to introduce a variety of functional groups to a polymer. Of the various techniques used for grafting, chemical grafting is generally reported to give higher graft levels and has efficiently been used to graft monomers like acrylamide on polyethylene oxide, methyl methacrylate (MMA) onto silk sericin, poly(ether glycol) methyl ether methacrylate on polyether sulfone, poly(N-phenylethylene diamine methacrylamide) on PS microplate and acrylamide on CFP.[21-26]

Glycidyl methacrylate (GMA) is an interesting monomer with pendant epoxy groups that directly reacts with sulfhydryl, amino and carboxyl groups to form stable covalent bonds with biomolecules.[27-32] The monomer has therefore been used for grafting and such epoxy-modified polymer surfaces have also been reported to be resistant against hydrolysis and stable during long storage periods.[33-36]

Dot-ELISA - a highly versatile solid phase immunoassay for antibody or antigen detection - has been widely employed in several serological tests because of its sensitivity and specificity in addition to being practical and less expensive diagnostic test, not requiring either sophisticated equipment or trained technical personnel.[37] The present paper aims at the evaluation and standardization of GMA grafted CFP (with GMA graft % from 10 to 100), developed and reported earlier by the same group of investigators, in dot-ELISA.[38] The paper also describes the practical application of CFP-g-GMA surfaces for identification of human blood and the source of mosquito blood meal (species on which mosquito fed).

## 2. Experimental

### 2.1 Materials

Glycidyl methacrylate (GMA), Bovine serum albumin (BSA), Tween-20, 4-chloro-1-naphthol and hydrogen peroxide ($H_2O_2$) were purchased from Sigma-Aldrich (USA) and used as received. The CFP (No. 393) used for grafting was obtained from Sartorious, Germany. Nitrocellulose membranes (0.45µm pore size) were supplied by Advanced Microdevices (pvt.), Ambala Cantt, India. Cerric ammonium nitrate, nitric acid, acetone and all other analytical grade chemicals were purchased from CDH, India. Immunoglobulins (Ig): Goat anti-rabbit (GAR IgG), rabbit anti-goat (RAG IgG), and horseradish peroxidase (HRP) conjugated to: GAR IgG, RAG IgG and rabbit anti-human (RAH) IgG were purchased from Bangalore Genei, India.

Mosquito blood meal samples of laboratory reared *A. stephensi* deliberately fed on human and buffalo host were taken from Malaria Research Centre (ICMR), New Delhi, India. Blood samples directly taken from human and buffalo were also provided by the same centre. All the buffers were prepared in Milli Q water. All samples prepared in % were taken w/v, unless otherwise stated.

### 2.2 Graft polymerization

Grafting of GMA monomer on CFP was carried out by chemical initiation using cerric ammonium nitrate (CAN) as an initiator. Grafting was undertaken in a glass ampoule under nitrogen atmosphere as detailed in earlier publication and represented in Scheme 1.[38] GMA grafted CFP was cut in thin strips to be used for dot-ELISA.

### 2.3 Characterization

GMA grafting on CFP was confirmed by various standard techniques ATR-FTIR, SEM and TGA analysis.[38] Thickness of the ungrafted and GMA grafted CFP samples were measured using an Essdiel Thickness gauge at 20 $gfcm^{-2}$ pressure.

### 2.4 Static lattice atomistic simulations

Molecular simulations were performed using commercial softwares: HyperChem™ 8.0.8 Molecular Modeling System (Hypercube Inc., Gainesville, Florida, USA) and ChemBio3D Ultra 11.0 (Cambridge Soft Corporation, Cambridge, UK). The structure of poly(GMA) was built in its syndiotactic stereochemistry as 3D model using ChemBio3D Ultra while the structure of the cellulose (CEL) was generated using the built-in polysaccharide builder module of HyperChem. The models were energy-minimized using a progressive-

convergence-strategy where initially the MM+ force field was used followed by energy-minimization using the Amber 3 (Assisted Model Building and Energy Refinements) force field. The conformer having the lowest energy was used to create the polymer-polymer complex. A complex of one polymer molecule with another was assembled by disposing the molecules in a parallel way, and the same procedure of energy-minimization was repeated to generate the final models: PGMA, CEL, CEL-CEL ($CEL_2$) and PGMA-$CEL_2$. Full geometry optimization was carried out in vacuum employing the Polak–Ribiere conjugate gradient algorithm until an RMS gradient of 0.001 kcal/mol was reached. For molecular mechanics calculations in vacuum, the force fields were utilized with a distance-dependent dielectric constant scaled by a factor of 1. The 1-4 scale factors were electrostatic 0.5 and van der Waals 0.5.[39]

### *2.4.1 Molecular mechanics assisted model building and energy refinements*

A molecular mechanics conformational searching procedure was employed to acquire the data employed in the statistical mechanics analysis, and to obtain differential binding energies of a Polak–Ribiere algorithm and to potentially permit application to polymer composite assemblies. MM+ is a HyperChem modification and extension of Norman Allinger's Molecular Mechanics program MM2, whereas AMBER is a package of computer programs for applying molecular mechanics, normal mode analysis, molecular dynamics and free energy calculations to simulate the structural and energetic properties of molecules.[40,41]

## 2.5 Evaluation and standardization of CFP-g-GMA surface for dot-ELISA with model system

GMA grafted CFP strips were dipped in PBS (pH 7.4) for 5 min and dried at 37°C for next 10 min. Various dilutions of RAG IgG (prepared in PBS) were spotted on to the strips as 2µL spots each, while PBS was used as control dot. The applied dots were allowed to air dry at 37°C for 20 min. Non-specific protein binding sites left on the strips were then blocked by incubating in 10 mL of blocking solution for 30 min at 37°C. Strips were then briefly washed in PBS-Tween (0.05%) to remove the blocking solution and thereafter incubated with 10mL of peroxidase labeled antispecies IgG conjugate (GAR IgG HRP) for 30 min at 37°C. The unbound conjugate was aspirated off and strips were washed with PBS-Tween for 30 s with gentle shaking. Finally, the strips were dipped in covered tray containing the freshly prepared 4-chloro-1-naphthol substrate solution: 6 mg of 4-chloro-1-naphthol dissolved in 2 mL

methanol and added to 8 mL PBS containing 100 µL of 3% $H_2O_2$ (v/v). Reaction was allowed to proceed for 5 min in the dark to develop the color, where after the enzyme reaction was stopped by washing with water. Positive results were indicated by the development of a purple-blue color on the spotted site. Sensitivity of the polymeric surfaces was evaluated by spotting serial dilutions of RAG IgG as model antibody in a concentration range from 200 $ngmL^{-1}$ to 6 $ngmL^{-1}$. Different blocking agents like ethanolamine, bovine serum albumin (BSA) and skimmed milk were tried in varied percentages for their efficacy to block the remaining non-specific sites. GAR IgG HRP-conjugate was used in dilutions ranging from 1:1000 to 1:5000. In order to optimize the time duration of the immunoassay, the incubation periods at various steps were varied from 15 min to 1 h. Specificity of the assay was tested using GAR IgG HRP-conjugate against RAG IgG and GAR IgG. Two concentrations (100 $ngmL^{-1}$ and 50 $ngmL^{-1}$) of both the antibodies were spotted onto the polymeric strip followed by the usual assay steps with standardized solutions.

### 2.6 Specimen of blood samples and preparation of elutes

Human and buffalo blood samples were taken and spotted on separate filter papers as 10 µL dots. The spotted specimen samples were dried at 37°C for one hour and then stored in desiccator at 4°C until further use. When required, a filter paper disc of 10 mm diameter was cut from the middle of a blood spotted specimen sample using a paper punch. All the blood spotted disc samples were then eluted in 100 µL of PBS, pH 7.4 at room temperature for 1h. Eluate thus obtained was serially diluted in PBS from 2 to 10,000-fold (1:1 to 1:10,000). Samples were also taken from different mosquitoes, which have fed either on human or buffalo, by quashing the mosquitoes onto the whatman filter paper no.1. Drying, storage, elution and dilution of mosquito blood meal samples taken on filter paper was done as mentioned above for other blood samples. Specificity test with human and buffalo blood and the identification of the source of mosquito blood meal was carried out at the best dilution identified with human blood sensitivity studies.

### 2.7 Dot-ELISA on CFP-g-GMA surface for identification of human blood and mosquito blood meal source

GMA grafted CFP strips were dipped in PBS solution for 5min and dried at 37°C for another 10 min. Micropipette was used to transfer various eluted blood samples (2 µL) onto the strips and air dried at 37°C for 20 min. Samples spotted on strips were washed with PBS-Tween

twice for 30 s each with gentle shaking. The strips were then incubated with 10 mL of 5% skimmed milk for 30 min for blocking nonspecific protein binding sites. After removing the blocking solution, strips were incubated with 10 mL of peroxidase labelled RAH IgG HRP-conjugate for 30 min at 37°C. The unbound conjugate was washed with PBS-Tween (30 s) at 37°C and the strips were dipped in dark in 10 mL of freshly prepared chloro-naphthol substrate solution and the reaction was stopped by washing with water. To determine the sensitivity of grafted CFP strips for human blood, the eluted and then serially diluted human blood samples were applied as 2 µL dots followed by above mentioned dot-ELISA steps. For the specificity test, RAH IgG HRP-conjugate was tested against eluates from human and buffalo blood samples taken separately. From both the type of blood samples (human and buffalo) two dilutions of the eluate (100 and 1000-fold) were spotted each of 2 µL, followed by above mentioned dot-ELISA steps.

Mosquito blood meal source identification with modified CFP surface was also carried out utilizing samples of mosquito blood meal of known source (human or buffalo). Blood meal eluate for spotting was used at 100-fold dilution and RAH IgG HRP-conjugate was used for detection.

## 3. Results and discussion

### 3.1 Graft polymerization

Grafting of GMA monomer on CFP was carried out by free radical polymerization using CAN as chemical initiator in aqueous medium. The probable reaction mechanism is presented in Scheme 1 and detailed studies of various parameters of grafting *i.e.* concentrations of monomer (1 to 10%) and initiator (1.0-6.0x$10^{-3}$ mol$L^{-1}$), the polymerization temperature (40-70ºC) and time (5-30 min) is reported in our earlier publication.[38] The degree of grafting of GMA onto cellulose filter paper varied from 10 to 102±3%, under different reaction conditions and a maximum of 102±3% was recorded at 60°C in 25 min with 4x$10^{-3}$ mol$L^{-1}$ of initiator (CAN) concentration and 5% GMA monomer.

### 3.2 Characterization

The GMA grafting was confirmed by chemical analysis of ungrafted and various grafted surfaces using ATR-FTIR. Apart from the characteristic absorptions of filter paper surface at 3400 and 2920 $cm^{-1}$ because of O-H stretching and C-H stretching vibrations respectively and at 1426 and 1023 $cm^{-1}$ of C-H bending and O-H bending respectively, the grafted surface

exhibited additional peaks characteristic of GMA (Fig. 1(a)). The peaks at 906 and 845 $cm^{-1}$ are assigned to epoxide group while the peak at 1730 $cm^{-1}$ corresponds to the carbonyl functional group of grafted GMA. The scanning electron micrographs showed an introduction of heterogeneity along and across the fibres which increased with the increase in graft level which may be the outcome of incompatibility of the hydrophobic poly(GMA) graft with the hydrophilic cellulosic filter paper matrix (Fig. 1(b)). The thickness of unmodified CFP was recorded as 0.19 mm which increased from 0.21 to 0.54 mm with an increase in the graft level from 10 to 100% (Fig. 1(c)).

### 3.3 MMER analysis

Molecular mechanics energy relationship (MMER), a method for analytico-methematical representation of potential energy surfaces, was used to provide information about the contributions of valence terms, noncovalent Coulombic terms, and noncovalent van der Waals interactions for polymer/polymer interactions. The MMER model for potential energy factor in various molecular complexes can be written as:

$$\mathbf{E_{molecule/complex}} = V_{\sum} = V_b + V_\theta + V_\varphi + V_{ij} + V_{hb} + V_{el} \quad ...(1)$$

where, $V_{\sum}$ is related to total steric energy for an optimized structure, $V_b$ corresponds to bond stretching contributions (reference values were assigned to all of a structure's bond lengths), $V_\theta$ denotes bond angle contributions (reference values were assigned to all of a structure's bond angles), $V_\varphi$ represents torsional contribution arising from deviations from optimum dihedral angles, $V_{ij}$ incorporates van der Waals interactions due to non-bonded interatomic distances, $V_{hb}$ symbolizes hydrogen-bond energy function and $V_{el}$ stands for electrostatic energy.

In addition, the total potential energy deviation, $\Delta E_{total}$, was calculated as the difference between the total potential energy of the complex system and the sum of the potential energies of isolated individual molecules, as follows:

$$\mathbf{\Delta E_{Total(A/B)}} = E_{\mathbf{Total}(A/B)} - (E_{\mathbf{Total}(A)} + E_{\mathbf{Total}(B)}) \quad ...(2)$$

$$\mathbf{E}_{GMA} = 543.925V_{\sum} = 2.444V_b + 511.545V_\theta + 27.634V_\varphi + 2.302V_{ij} \quad ...(3)$$

$$\mathbf{E}_{CEL} = -4.641V_{\sum} = 1.477V_b + 8.718V_\theta + 6.145V_\varphi + 13.110V_{ij} - 34.094V_{el} \quad ...(4)$$

$$\mathbf{E}_{CEL2} = -20.212V_{\sum} = 1.404V_b + 8.624V_\theta + 7.617V_\varphi + 4.778V_{ij} - 42.036V_{el} \quad ...(5)$$

$\mathbf{E}_{GMA\text{-}CEL2}$=475.869$V_{\sum}$ =5.275$V_b$+ 526.026$V_\theta$+ 44.213$V_\varphi$ -9.053$V_{ij}$ -90.592$V_{el}$ ...(6)

$\mathbf{\Delta E}$ = -47.844kcalmol$^{-1}$

The molecular stability can then be estimated by comparing the total potential energies of the isolated and complexed systems. If the total potential energy of the complex is smaller than the sum of the potential energies of isolated individual molecules in the same conformation, the complexed form is more stable and its formation is favoured.[42]

### *3.3.1 Formation of polymeric assemblies*

The GMA was modeled as a polymer - PGMA - with monomer chain length of 4 monomer contents for better efficiency in terms of computational time and modeling space. The cellulose based polysaccharide platform was built by modeling two parallel cellulose chains with 4 oligosaccharide contents in each chain. The energetic profiles of the formation of the polymeric assemblies viz. CEL-CEL ($CEL_2$) and PGMA-$CEL_2$, in vacuum, are represented by energy equations 3-6 and the conformational profile for the same are depicted in Fig. 2. The energy equations demonstrated that the polymeric systems were highly stabilized in terms of respective bonding and non-bonding energy factors. The energy stabilization with negative steric energies in all case of PGMA-$CEL_2$ suggested good compatibility and reactivity. Additionally, the geometric conformation and the hydrogen bonding suggest the involvement of C3-C2 bond of cellulose with the reactive functionalities of PGMA. The geometric stabilization displayed $\Delta$E~-48 kcalmol$^{-1}$ wherein the PGMA-$CEL_2$ complex was destabilized by all bonding energy contributions viz. bond stretching, bond angle and torsional constraints and stabilized by van der Waals forces and electrostatic interactions (non-bonding interaction). Strikingly, introduction of the acrylic polymer introduced deviations from optimum dihedral angles and bond positions with values in the range of ~2 kcalmol$^{-1}$ to ~10 kcalmol$^{-1}$ which lead to a highly strained molecular geometry. This may explain the experimental observation "heterogeneity along and across the fibres with an increase in graft level which may be the outcome of incompatibility of the hydrophobic poly(GMA) graft with the hydrophilic cellulosic filter paper matrix". However, the van der Waals interactions (~-15 kcalmol$^{-1}$) and electrostatic contributions (~-50 kcalmol$^{-1}$) added to the stabilization and retrieved high negative values which may be due to PGMA acting as filler in the space lattice of the binary system (Fig. 2). This in turn explains the notion of "an increase in adsorption properties of CFP with grafted GMA" as predicted in the experimental

discussion. Furthermore, a close look at the molecular complex reveals the presence of both inter- and intra-molecular H-bonding. These non-bonding interactions, from van der Waals forces to electrostatic contributions, may be due to the hydrophobic interactions arising from the inclusion of PGMA which can further provide covalent attachment to the antibodies through the epoxy groups, not involved in the bonding with CEL, leading to the applicability of PGMA-CEL as a potential substrate for evaluation in ELISA.

### 3.4 Evaluation and standardization of CFP-g-GMA surface for dot-ELISA with model system

For a reliable immunoassay there has to be a balance between sensitivity, background noise and specificity of the solid phase. Sensitivity of a matrix broadly depends on the surface binding efficacy of the antigen/antibody, blocking condition (type and amount of blocking agent) and the concentration of the conjugate used. A model system was designed using RAG, GAR immunoglobulins and their corresponding HRP-conjugates to standardize the dot-ELISA assay on the modified CFP polymeric surface.

#### *3.4.1 Effect of blocking agent*

Prevention of non-specific binding of reagents to the matrix is important for a solid phase immunoassay. Blocking of all protein-binding sites left on the surface after sample spot application is important and achieved using a proper blocking agent in an appropriate amount as insufficient blocking may result in a high background while over-blocking may decrease the sensitivity. For a novel surface before proceeding for immune reaction, its important to standardize the blocking condition (type and amount of blocking agent). Three different blocking agents had been investigated in varying percentages (1%, 2% and 5%) for their efficiency in blocking GMA grafted CFP surface and the results are presented in Fig. 3(a). Ethanolamine, a commonly employed blocking agent for the epoxy groups (present in grafted GMA on CFP), was able to block the surface partially. A better signal to noise ratio was observed at an ethanolamine amount of 1%. For all the concentrations of ethanolamine used, a background noise was always present, which was higher for modified CFP with low grafting level. Although ethanolamine is able to react with and block the non-specific GMA sites present on the grafted CFP, it is not equally effective for the blocking of cellulosic component of the matrix. This results in background noise when ethanolamine is used as a blocking agent. BSA, as a blocking agent gave a better signal to noise ratio than

ethanolamine, and was best at a usage of 2%. These results indicate BSA as a better blocking agent than ethanolamine for both GMA and cellulose. Although, BSA is generally used for blocking NC membrane – the widely used membrane for dot-ELISA, its blocking effect on GMA grafted CFP was although not very profound but, satisfactory. The signals (colored dots) obtained with different percentages of skimmed milk were almost comparable but, a higher background noise was observed with 1% skimmed milk, which reduced with an increase in amount to 2%. Further increase in skimmed milk amount to 5% was able to block the surface completely without dampening the color dot intensity. This established skimmed milk as the best blocking agent for the GMA grafted CFP surface at a concentration of 5%.

### *3.4.2 Effect of conjugate dilution*

The conjugate in dot-ELISA is almost always antibody linked to an enzyme. The antibody is specific to and probes for the analyte of interest in the sample spot while the linked enzyme in conjugate finally produces a visible signal with chromogenic substrate. A balanced concentration of enzyme conjugate is required because increase in conjugate concentration to attain higher sensitivity can lead to higher background and reduced specificity. Conjugate (GAR IgG–HRP) was therefore diluted to various extents ranging from 1:1000 to 1:5000, in order to determine the optimal dilution for the system under investigation. All the dilutions were used in combination with all the three blocking agents at their best blocking concentration (%) determined in previous section (3.4.1). Conjugate dilutions showed different results with different blocking agent for detecting various concentrations of RAG IgG antibody spotted as sample on CFP-g-GMA. The cumulative effect of HRP-conjugate dilutions with ethanolamine, BSA and skimmed milk as blocking agent has been shown in Fig. 3(b) (i-iii). With ethanolamine (1%) blocked surfaces, the conjugate dilution of 1:1000 to 1:5000 gave more or less similar results in terms of the lower limit of the analyte (RAG-IgG) detected (25 $ngmL^{-1}$). It is assumed that the lower dilutions of 1:1000 and 1:1500 would have been able to identify and generate signals for even lower antibody concentrations, but, due to increased background noise at these dilutions, the positive signals (colored dots) were not visible. At an increased dilution of 1:2000, the background noise decreased and the signal intensity remained comparable, while, a further dilution of 1:5000 reduced the intensity of signals (Fig. 3(b)-i). BSA (2%) blocked CFP-g-GMA strips gave a higher background noise at a conjugate dilution of 1:1000 which decreased progressively on further dilution from 1:1500 to 1:5000. As with ethanolamine blocked surfaces, the positive signals on strips

incubated with 1:1000 conjugate dilution were visible only at higher analyte concentration spots (Fig. 3 (b)-ii). Due to an added effect of increase in conjugate dilution and better BSA blocking much of the background noise was reduced at a dilution of 1:1500 and 1:2000. The colored spots were visible for spotted antibody concentration of 12 $ngmL^{-1}$, although the intensity of these dots was low. When skimmed milk (5%) blocked CFP-g-GMA surfaces were evaluated in combination with conjugate dilutions, a significant advance in signal to background noise was observed at a dilution of 1:1500 and a clear background was obtained at dilutions above 1:2000 (Fig. 3 (b)-iii). As seen in figure, the color intensity of dots remained comparably same upon increase in dilution from 1:1500 to 1:2000 but on further dilution to 1:5000 the intensity decreased.

### *3.4.3 Sensitivity*

The visibility of a dot depends on the contrast of the color generated against the background and is thus dependent on the concentration of analyte in a sample spot. The sample is therefore applied in small volumes of concentrated analyte and the minimum detectable concentration i.e. sensitivity of any assay system is determined by applying serial dilutions of the analyte. The GMA grafted CFP with different percent grafting were therefore evaluated for their sensitivity by using antibody (RAG-IgG) dilutions from 200 to 6 $ngmL^{-1}$ in combination with various blocking agents (used at varied concentrations) and conjugate dilutions. The cumulative influence of reagents on the detection of antibody spots of different concentrations applied onto the surface of CFP-g-GMA is shown in Fig. 3(b). With ethanolamine (1%) as a blocking agent, the highest sensitivity recorded is 25 $ngmL^{-1}$ with fairly clear background at a conjugate dilution of 1:2000. Although the sensitivity remained comparably same at a higher dilution of 1:5000, the color intensity of the dots weakened (Fig. 3(b)-i). When BSA (2%) was used as a blocking agent the same conjugate dilution of 1:2000 showed improved sensitivity and was able to detect the antibody spot of 12 $ngmL^{-1}$, although the color intensity of the dots was very low. This established BSA as a better blocking agent than ethanolamine, for CFP-g-GMA surfaces at a conjugate dilution of 1:2000. On increasing the conjugate dilution to 1:5000 a decline in the sensitivity of the surface was recorded. (Fig. 3(b)-ii). Skimmed milk at a concentration of 5% effectively blocked the non-specific sites on the modified CFP and gave the best signal to noise ratio when used in combination with conjugate diluted to 1:2000. With this set of reagents the intensity of color developed for RAG-IgG concentration of 200 $ngmL^{-1}$ down to 12 $ngmL^{-1}$ were strong and very clearly

visible on the surface of modified CFP (Fig. 3(b)-iii). The signals at 6 $ngmL^{-1}$ antibody concentration were although weak but detectable and visible against the clear background of the developed matrix. The optimized assay protocol for dot-ELISA on GMA grafted CFP therefore required 5% skimmed milk as the blocking agent, a peroxidase labeled antispecies IgG conjugate diluted 2000 times and the standardized incubation period of 30 min in each step. Under these conditions the sensitivity of the surface observed was 6 $ngmL^{-1}$.

The results of the assay performed on modified CFP, with varying degree of grafting (ranging 10-100%), in accordance to the standardized and established dot-ELISA protocol is presented in Fig. 3(c). As seen in this figure, no defined color dots developed on the CFP surface with grafting level as low as 10%, instead the whole strip takes up the color. On an increase in grafting level to 20%, the color dots become visible but show a diffused boundary, which becomes defined only on the GMA grafted CFP with graft level above 20%. Although the dots with clear boundaries are visible on modified CFP with graft level of 40 to 60%, the dots obtained are larger. A progressive decrease in the size of the dots is observed with an increase in graft level from 40 to 70%, showing confined and sharp dots on modified CFP with GMA graft level of 70% and above. This observation can be explained by the varying protein binding ability of the modified CFP surface with varying graft levels of GMA. The grafted GMA is believed to alter the adsorption properties of CFP on one hand while providing covalent attachment to the antibodies on the other. Since the antibody binding properties of CFP with lower graft level is low, the antibody migrates with the buffer and on color development with the substrate, either the complete matrix takes up the color or larger dots are observed. Additionally, because of the diffusion of sample antibody to larger areas the color intensity dampens. Modified CFP with higher graft level exhibit higher antibody binding properties as can be seen from the development of compact and defined dots (Fig. 3(c)). Best results are visible at the CFP-g-GMA surface with 70% graft level. The surface show good intensity color dots due to the confinement of spotted antibody solution to a smaller region and thus gives the best signal to noise ratio which is comparable to that on standard NC membrane. Good results obtained with GMA grafted CFP at 70% graft level can be explained due to the optimum balance attained between the hydrophobic grafted GMA and hydrophilic properties of the cellulosic matrix, which makes the GMA grafted CFP a suitable matrix for dot-ELISA. Moreover, GMA grafted on CFP provides partial covalent attachment to the antibodies through its active epoxy group and also introduces hydrophobicity to the surface which controls the excessive wicking action of the CFP matrix. The level of

hydrophilicity and adsorption capacity present at 70% GMA grafted CFP due to the inherent hydrophilic property of CFP backbone is sufficient in providing better diffusion of antibodies to the matrix. It may also have a role in building a hydrophilic microenvironment around the hydrophobic GMA in order to maintain the conformational stability of the antibodies attached to CFP-g-GMA matrix. On increase in graft level beyond 80% the background noise reappears; this reduces the dot visibility especially at lower antibody concentrations. This background noise may be attributed to the incomplete blocking due to the highly hydrophobic nature of the surface (at 100% graft level) which hinders the diffusion of the blocking agent to the active sites of the matrix.

The GMA grafted CFP with 70% graft level was therefore established as the best and most appropriate matrix for the dot-ELISA at optimized and standardized conditions of: 5% skimmed milk blocking agent, a peroxidase labeled antispecies IgG conjugate diluted 2000 times and the standardized incubation period of 30 min in each step. The developed matrix has also been compared with the conventionally used NC membrane for dot-ELISA in Table 1. All further experiments were carried out with 70% GMA grafted CFP matrix and the results of all dot-ELISA experiments undertaken with the model system are presented on this surface only.

### *3.4.4 Specificity*

Dot-ELISA specificity test with 70% GMA grafted CFP matrix were conducted for GAR IgG HRP-conjugate against RAG IgG and GAR IgG and the results are presented in Fig. 3(d). As can be seen, the color development was clearly observed on both the spots (50 and 100 $ngmL^{-1}$) of RAG IgG while there was no color development with GAR IgG. The result obtained is as expected because GAR IgG HRP conjugate used is complementary to RAG IgG and therefore binds specifically to RAG IgG only and not GAR IgG. This confirms the specificity of the CFP-g-GMA surface, showing no cross reactivity.

## 3.5 Dot-ELISA for detection of human blood

### *3.5.1 Sensitivity*

The results of the sensitivity (lowest detectable limit) of the CFP-g-GMA surface for human blood (antibodies present in human blood) are given in Table 2 and shown in Fig. 4. The RAH IgG HRP-conjugate was used which specifically binds to human antibodies. The human

blood eluate dilutions ranging from 10 to 100-fold gave strong positive results while any further dilution dampened the color intensity of the dots and finally showed no result at a dilution of 1:10,000. Although the color intensity of dots obtained with neat eluate and that of 2-fold diluted eluate was good, the dots obtained with these eluates were diffuse. This diffuse dot formation may be the result of the presence of higher concentration of antibodies in the sample. The results thus established that a 0.1µL dot of blood on filter paper disc, eluted with 100 µL of PBS is sufficient to be identified through dot-ELISA on the developed GMA grafted CFP matrix. The sensitivity results of developed matrices with human blood have been compared to that of the commercially used NC membrane, which shows an absolute correlation (Fig. 4).

### *3.5.2 Specificity*

RAH IgG HRP-conjugate was used for the specificity test against human and buffalo blood eluates. Results in Fig. 5(a) show good color intensity dots at both spots of blood eluate (1:100 and 1:1000 diluted) obtained from human and no color development with either of the two buffalo blood eluted spots. The results obtained are as predicted because the conjugate (RAH) has been specifically used against human blood which identifies human antibodies only and does not bind to antibodies from any other organism. This confirms that there is no non-specific reaction to other species' blood samples (eluates). Blood eluate samples from human and buffalo were spotted in replica (n=2) in order to confirm the reproducibility.

### 3.6 Dot-ELISA for detection of mosquito blood meal source

Fig. 5(b) shows the result of identification of source of mosquito blood meal. The blood meal eluate obtained from mosquitoes that have fed on three different human were applied as sample 1, 2 and 3, while the ones fed on two different buffalos were used as sample 4 and 5. Out of all spotted samples only 1, 2 and 3 were identified (by colored dot formation), with RAH IgG HRP-conjugate, which correspond to the blood meal obtained from mosquitoes that fed on humans. The conjugate used is anti to human antibodies and therefore, specifically binds to and identifies human antibodies only. The blood meal eluates of mosquitoes fed on buffalo did not give a positive result thereby showing no color dots in Fig. 5(b) for sample 4 and 5. Thus, the GMA grafted CFP matrix successfully identified the mosquito blood meal source.

## 4. Conclusion

GMA grafted CFP molecular mechanics simulations and in silico energy minimizations demonstrated the involvement of C3-C2 bond of cellulose in reaction with the GMA molecule resulting in a stabilized structure of the matrix. The GMA grafted CFP with varying graft level ranging from 10-100% were evaluated for application in dot-ELISA through a model system. The standardized conditions established for carrying out the assay on grafted CFP were: 5% skimmed milk as blocking agent, a peroxidise labelled antispecies IgG conjugate diluted 2000 times and the optimized incubation period of 30 min in each step. Under these conditions, a minimum background noise and the highest sensitivity of 6 $ngmL^{-1}$ was recorded at 70% GMA grafted CFP matrix. This standardized CFP-g-GMA (70% graft level) surface and protocol when applied for detection of human antibody in blood by direct ELISA method using blood eluate as sample dots showed that 10 µL dot of blood on whatman filter paper no. 1 eluted with 100 µL PBS gave the best intensity of colored dots although elution with 1000 µL PBS also gave a good intensity. The same graft level was successfully used to identify the source of mosquito blood meal, an important parameter in epidemiological studies, particularly in determining the role of the mosquito in malaria transmission. Therefore, modified CFP with 70% GMA graft level was highly specific as dot-ELISA matrices, showing no non-specific reactions either in a model system or with blood samples. The surface is equally sensitive and specific as nitrocellulose membrane with added advantage of being biodegradable, ecofriendly, many folds less expensive, easier to handle and does not require any special preparation for covalent binding of biomolecules. The prepared surfaces are being explored by the research group for quantitative ELISA and the results are encouraging. The present investigation established the developed surface to possess a strong potential to be used as matrix in dot-ELISA for detection of various diseases to be performed in the field conditions and in minimally equipped laboratories.

## References


1 E. Engvall and P. Perlmann, *Immunochemistry*, 1971, **8**, 871-874.

2 G. C. Le Goff, B. P. Corgier, C.A. Mandon, G. De Crozals, C. Chaix, L. J. Blum and C. A. Marquette, *Biosens. Bioelectron.*, 2012, 35, 94-100.

3 A. M. Pinheiro, M. F. Costa, B. Paule, V. Vale, M. Ribeiro, I. Nascimento, R. E. Schaer, M. A. O. Almeida, R. Meyer and S. M. Freire, *Veterinary Parasitol.*, 2005, **130**, 73-79.

4 H-B. Hong, H-J. Krause, K-B. Song, C-J. Choi, M-A. Chung, S. Son and A. Offenhäusser, *J. Immunol. Methods*, 2011, **365**, 95-100.

5 O. P. Lehtonen and M. K. J. Viljanen, *J. Immunol. Methods*, 1980, **34**, 61-70.

6 J. M. Kogot, D. A. Sarkes, I. Val-Addo, P. M. Pellegrino and D. N. Stratis-Cullum, *Biotechniques*, 2012, **52**, 95-102.

7 F. Boudet, J. Theze and M. Zouali, *J. Immunol. Methods*, 1991, **142**, 73-82.

8 F. B. Bouche, E. Schecklies and C. P. Muller, *Clin. Chem.*, 2002, **48**, 378-380.

9 C. Westblad, Y. A. Levendis, H. Richter, J. B. Howard and J. Carlson, *Chemosphere*, 2002, **49**, 395-412.

10 B. Feng, Y. Dai, H. Zhang, L. Wang, Y. Ding and H. Zeng, *J. Immunoassay Immunochem.*, 2009, **30**, 457-466.

11 N. Suzuki, M. S. Quesenberry, J. K. Wang, R. T. Lee, K. Kobayashi and Y. C. Lee, *Anal. Biochem.*, 1997, **247**, 412-416.

12 S. M. L. Montenegro, J. D. B. Silva, M. E. F. B. Brito and L. B.Jr. Carvalho, *Revista da Sociedade Brasileira de Medcina Tropical*, 1999, **32**, 139-143.

13 X. Wang, T. Hagiwara, S. Uchiyama, *Ana. Chim. Acta*, 2007, **587**, 41-46.

14 M. Chellapandian, C.A. Sastry, *Bioprocess. Eng.*, 1994, **11**, 17-21.

15 M. Chellapandian and M. R. V. Krishnan, *Process. Biochem.*, 1998, **33**, 595-600.

16 Kh.M. Mostafa, *J. Appl. Polym. Sci.*, 2005, **5**, 341-346.

17 M. Yasuzawa, K. Edagawa, T. Matsunaga, H. Takaoka and T. Yabutani, *Anal. Sci.*, 2011, **27**, 337-340.

18 A. D. Barbosa, F. S. M. de Barros, E. Q. Callou, A. M. P. Almeida, A. M. Araujo, W. M. Azevedo and L. B. Jr. Carvalno, *Mem. Inst. Oswaldo. Cruz.*, 2000, **95**, 95-96.

19 N. Strömberg, E. Mattsson and A. Hakonen, *Anal. Chimica Acta*, 2009, **636**, 89-94.

20 A. Afshar, P. F. Wright and G. C. Dulac, *J. Clin. Mirobiol.*, 1986, **3**, 563-567.

21 S. R. Shukla and A. R. Athalye, *J. Appl. Polym. Sci.*, 1994, **54**, 279-288.

22 S. A. Agnihotri and T. M. Aminabhavi, *Int. J. Pharm.*, 2006, **324**, 103-115.

23 Y. Song, Y. Jin D. Wei and J. Sun, *J. Macro. Sci. Part A*, 2006, **43**, 899-907.

24 J. Peng, Y. Su, Q. Shi, W. Chen and Z. Jiang, *Bioresour. Technol.*, 2011, **102**, 2289-2295.

25 M. Akbulut, D. Lakshmi, M. J. Whitcombe, E. V. Piletska, I. Chianella, O. Güven and S. A. Piletsky, *ACS Comb. Sci.*, 2011, **13**, 646-652.

26 R. Tankhiwale and S. K. Bajpai, *Colloids Surf. B Biointerfaces*, 2009, **69**, 164-168.

27 S. P. Colowick and N. O'Kaplan, *Methods Enzymol.*, 1976, **44**, 32.

28 W. F. Gum, W. Riese and H. Ulbrich, Reacitous Polymer, Carl Hauser (1992) New York.

29 M. Y. Arica, *J. Appl. Polym. Sci.*, 2000, **77**, 2000-2008.

30 S. Edmondson and W. T. S. Huck, *J. Mater. Chem.*, 2004, **14**, 730-734.

31 Y. Liu, V. Klep, B. Zdyrko and I. Luzinov, *Langmuir*, 2004, **20**, 6710-6718.

32 E. L. Pfaunmiller, M. L. Paulemond, C. M. Dupper and D. S. Hage, *Anal. Bioanal. Chem.*, 2013, **405**, 2133–2145.

33 G. Bayramoğlu, S. Akgol, A. Bulut, A. Denizli and M. Y. Arica, *Biochem. Eng. J.*, 2003, **14**, 117-126.

34 A. Alberti, P. Fuochi, M. Guerra, D. Macciantelli, G. Torri, A. Valerio and E. Vismara, *Org. Biomol. Chem.*, 2011, **9**, 3199-3204.

35 M. H. Kunita, M. R. Guilherme, L. C. Filho, E. C. Muniz, E. Franceschi, C. Dariva and A. F. Rubira, *J. Coll. Interface Sci.*, 2011, **361**, 331-337.

36 A.W. Eckert, D. Gröbe and U. Rothe, *Biomaterials*, 2000, **21**, 441-447.

37 C. Tyagi, L. Tomar and H. Singh, *Anal. Chimica Acta***,** 2009, **632**, 256-265.

38 C. Tyagi, L. K. Tomar and H. Singh, *J. Appl. Pol. Sci.*, 2009, **111**, 1381-1390.

39 P. Kumar, V. Pillay, Y. E. Choonara, G. Modi, D. Naidoo and L. C. Toit, *Int. J. Mol. Sci.*, 2011, **12**, 694-724.

40 D. C. Warhurst, J. C. Craig, I. S. Adagu, D. J. Meyer and S. Y. Lee, *Malaria J.*, 2003, **2**, 26-40.

41 D. A. Pearlman, D. A. Case, J. W. Caldwell, W. S. Ross, T. E. Cheatham, S. De-Bolt III, D. Ferguson, G. Seibel and P. Kollman, *Comp. Phys. Commun.*, 1995, **91**, 1-3.

42 B. Y. Yu, J. W. Chung and S.-Y. Kwak, *Environ. Sci. Technol.*, 2008, **42**, 7522-7527.

## Schemes

**Scheme 1** Reaction scheme of grafting of GMA on CFP (a) activation of cellulose filter paper surface, (b) Grafting of GMA

## Table Captions

**Table 1** Comparison of developed and conventionally used dot-ELISA matrix

**Table 2** Sensitivity test with human blood

## Figure Captions

**Fig. 1** Characterzation: (a) FTIR spectra of (i) ungrafted CFP and (ii-v) GMA-grafted CFP with varying grafting percentage [(ii) 20%; (iii) 50%; (iv)70%; (v) 100%](Tyagi et al., 2009b); (b) Scanning electron micrographs of (i) ungrafted CFP and (ii-iv) GMA-grafted CFP with varying percent grafting [(ii) 20%; (iii) 70%; (iv) 100%](Tyagi et al., 2009b); (c) Effect of grafting on thickness of cellulose filter paper

**Fig. 2** Visualization of geometrical preferences of (a) PGMA; (b) CEL-CEL; and (c) PGMA-$CEL_2$ (d) 3-D connolly molecular structure of PGMA-$CEL_2$ matrix in transparent display mode after molecular simulation in vacuum. Color codes: C (cyan), O (red), and H (white).

**Fig. 3** Dot-ELISA studies with model system: (a) Effect of different blocking agents; (b) Effect of conjugate dilutions on RAG-IgG spotted CFP-g-GMA surface blocked with (i) ethnolamine (1%) (ii) BSA (2%), (iii) skimmed milk (5%); (c) Dot-ELISA comparison on cellulose filter paper with different graft level of GMA (under standardized condition); (d) Specificity test on CFP-g-GMA surface (70% graft level)

**Fig. 4** Sensitivity test on CFP-g-GMA surface (70% graft level) with human blood

**Fig. 5** Identification of (a) human blood and (b) mosquito blood meal

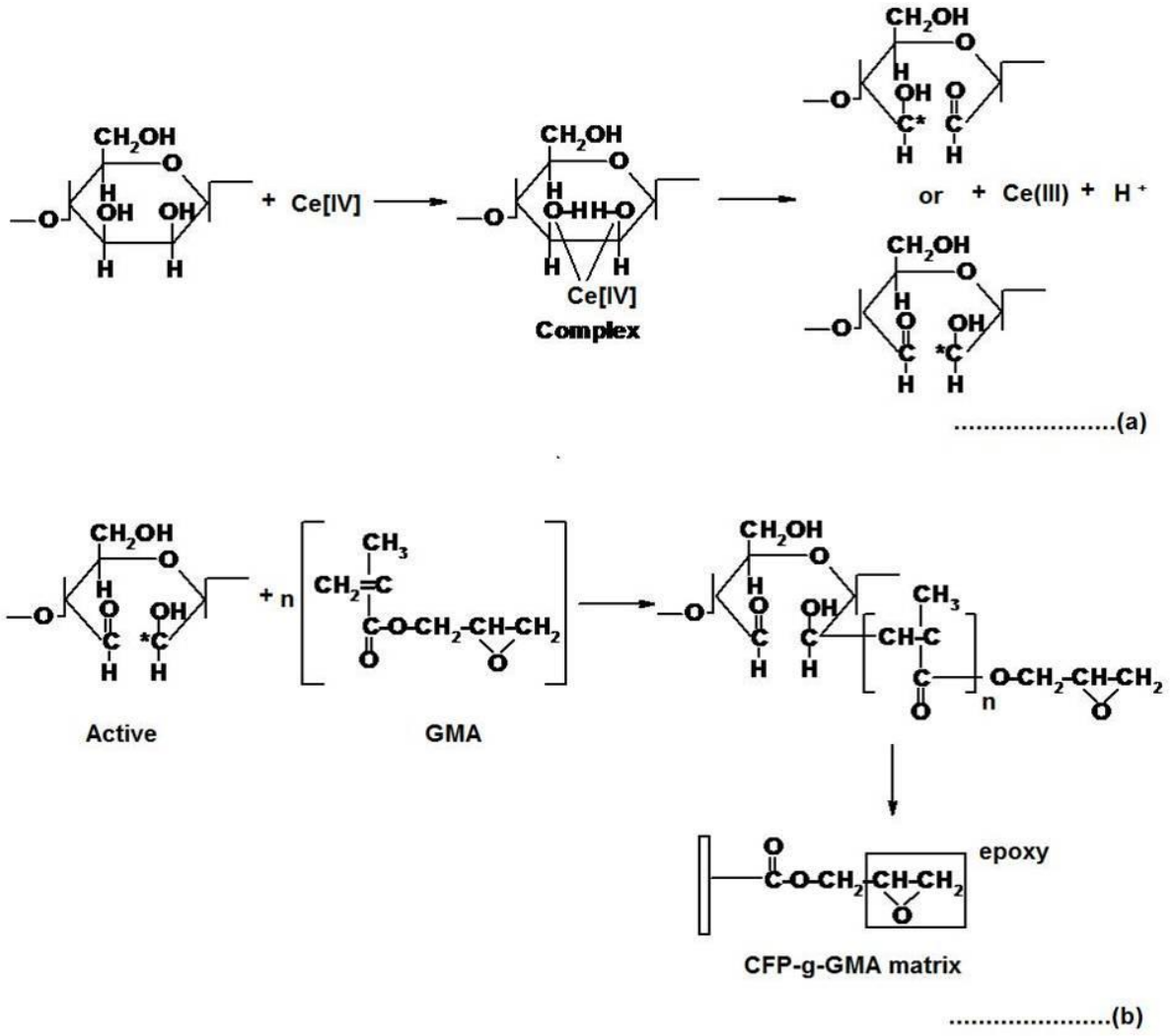


**Scheme 1**

**Table 1**

| Property | Developed system (GMA grafted CFP) | Conventionally used system (nitrocellulose membrane) |
|---|---|---|
| Sensitivity | Good | Good |
| Specificity | Good | Good |
| Time duration | | |
| Incubation | 30 min | 45 min |
| Total assay time | 1h 30 min | ~3 h |
| Washing | Very short /twice (~30 s each) | Extensive/thrice (1-2 min each) |
| Photostability | Stable | Unstable |
| Handling | Easy | With care |
| Cost | Economic | Costly |

**Table 2**

| Dilution of blood eluate | Sensitivity |
|---|---|
| Neat eluate | ++ |
| 1:1 | ++ |
| 1:10 | +++ |
| 1:100 | +++ |
| 1:1000 | + |
| 1:10,000 | - |

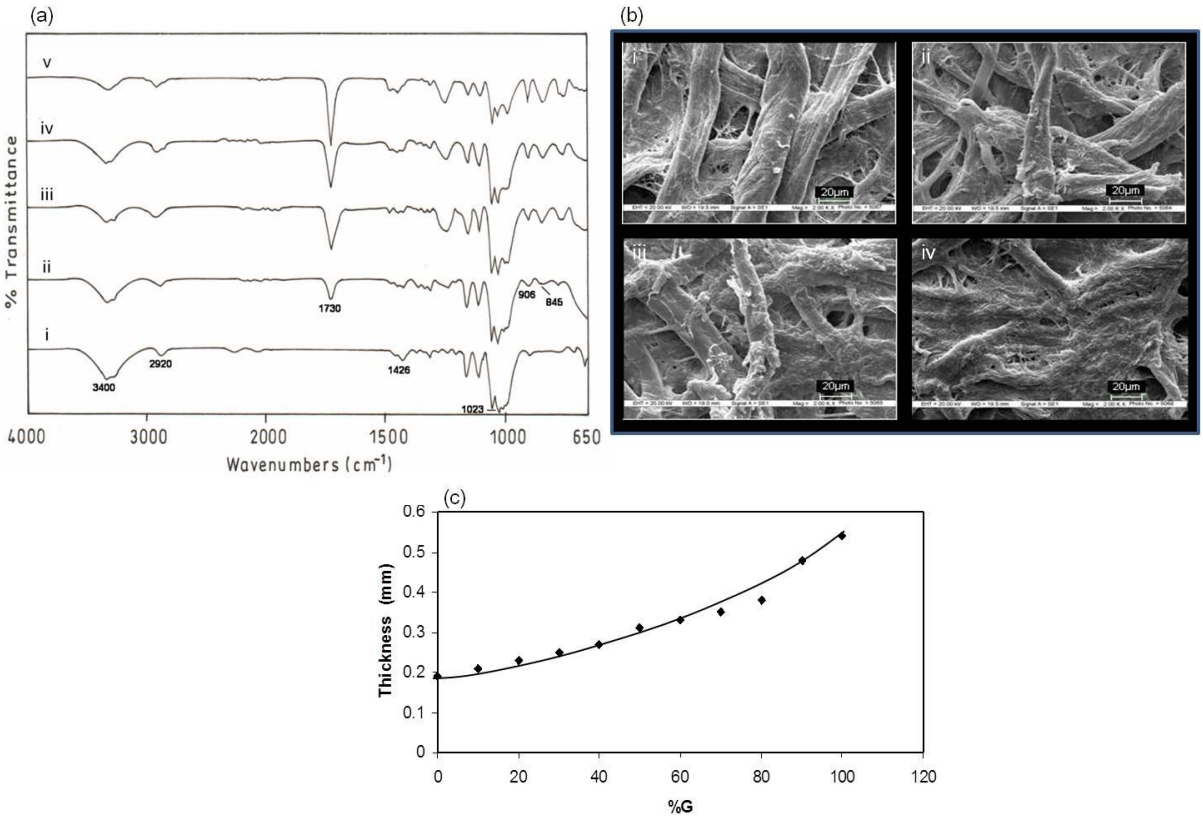


Figure 1

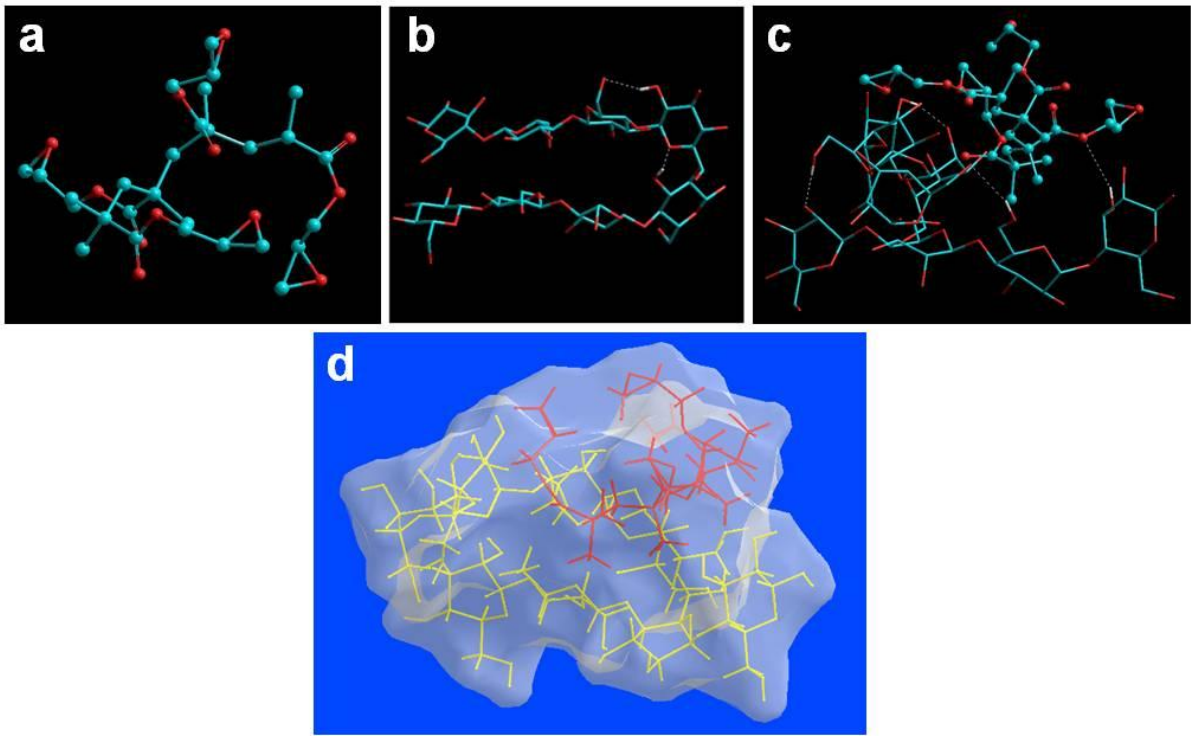


Figure 2

(a)

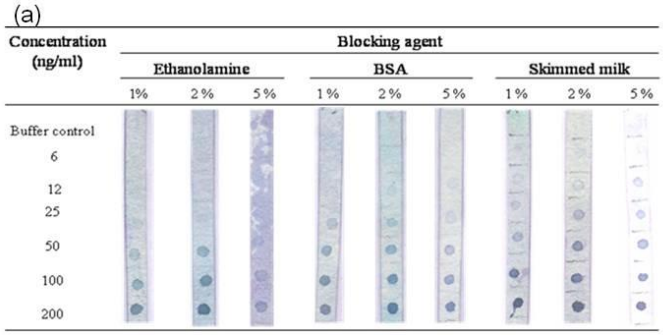


(b)

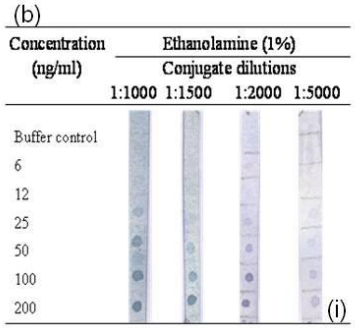


(c)

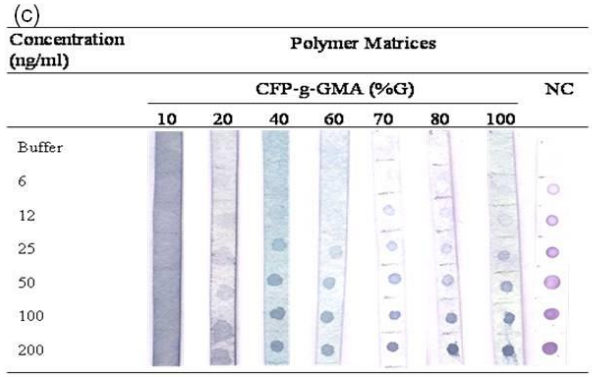


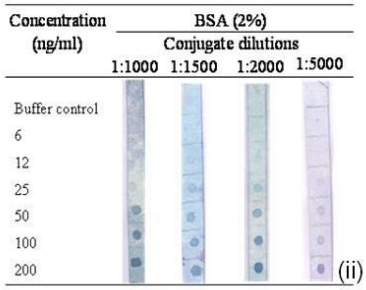


(d)

| Antibody | Antibody Conc. (ng/ml) | Antibody Conjugate | CFP-g-GMA (70%) |
|---|---|---|---|
| RAG-IgG | 100 | GAR-IgG-HRP | |
| | 50 | GAR-IgG-HRP | |
| GAR-IgG | 100 | GAR-IgG-HRP | |
| | 50 | GAR-IgG-HRP | |

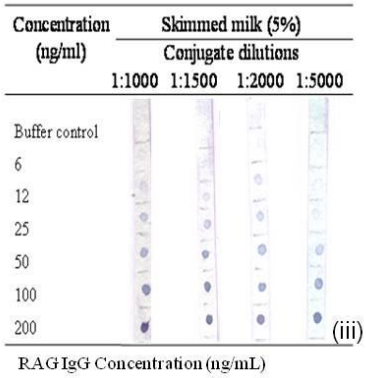

(a)

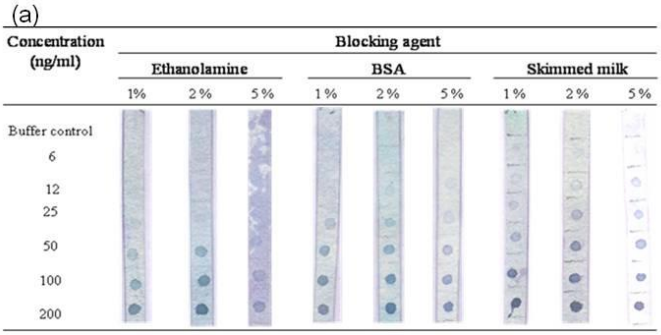


(b)

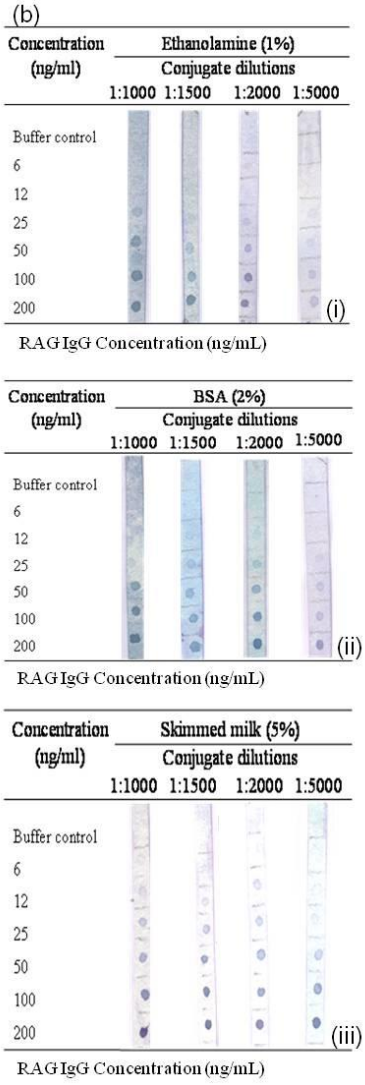


(c)

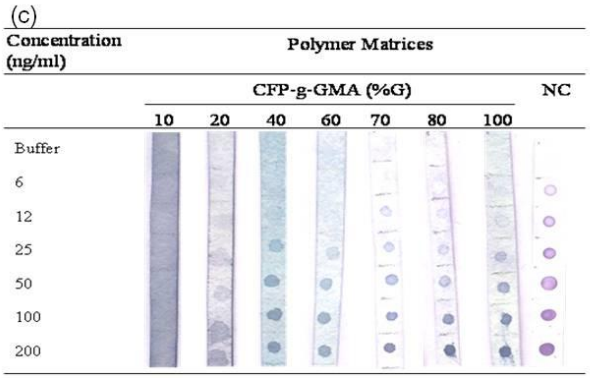


(d)

| Antibody | Antibody Conc. (ng/ml) | Antibody Conjugate | CFP-g-GMA (70%) |
|---|---|---|---|
| RAG-IgG | 100 | GAR-IgG-HRP | |
| | 50 | GAR-IgG-HRP | |
| GAR-IgG | 100 | GAR-IgG-HRP | |
| | 50 | GAR-IgG-HRP | |

Figure 3

| Dilution of Blood Eluate | Solid Phase (Matrix) | |
|---|---|---|
| | CFP-g-GMA (70%) | NC |
| Neat eluate | 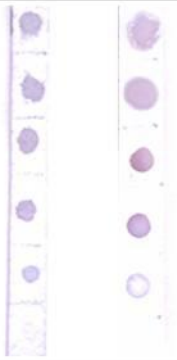 | |
| 1:1 | | |
| 1:10 | | |
| 1:100 | | |
| 1:1000 | | |
| 1:10,000 | | |

Figure 4

(a)

| Blood Source | Blood Eluate Dilution | Antibody Conjugate | CFP-g-GMA (70%) |
|---|---|---|---|
| Human | 1:100 | RAH-IgG-HRP |  |
| | 1:1000 | RAH-IgG-HRP | |
| Buffalo | 1:100 | RAH-IgG-HRP | |
| | 1:1000 | RAH-IgG-HRP | |

(b)

| Sample No. | Mosquito Blood Meal Source (Dilution of 1:100) | Conjugate | CFP-g-GMA (70%) |
|---|---|---|---|
| 1 | Human | RAH-IgG-HRP |  |
| 2 | Human | RAH-IgG-HRP | |
| 3 | Human | RAH-IgG-HRP | |
| 4 | Buffalo | RAH-IgG-HRP | |
| 5 | Buffalo | RAH-IgG-HRP | |

Figure 5

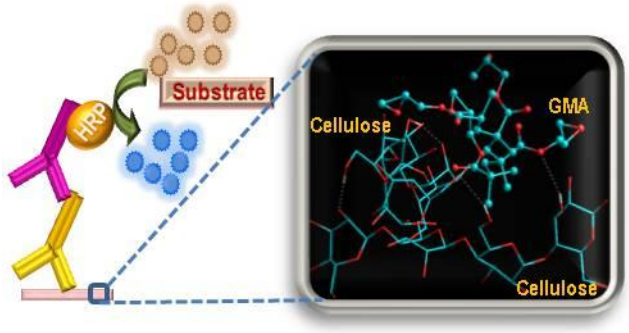


Graphical Abstract